

CORE-SHELL MODELLING OF AUXETIC INORGANIC MATERIALS

VICTOR ZAMMIT¹, RUBEN GATT¹, DAPHNE ATTARD¹
AND JOSEPH N. GRIMA^{1,2}

¹*Metamaterials Unit, Faculty of Science, University of Malta
Msida MSD 2080, Malta*

²*Department of Chemistry, Faculty of Science, University of Malta
Msida MSD 2080, Malta*

(Received 15 January 2014; revised manuscript received 8 March 2014)

Abstract: This paper investigates the suitability of the General Utility Lattice Program (GULP) for studying auxetic materials at the molecular level. GULP is a force-field based molecular modelling package which incorporates the ‘core-shell’ model for simulating polarisability. A validation procedure was performed where the capability of GULP to reproduce the structural and mechanical properties of SOD (a zeolite for which the single crystalline elastic constants have been experimentally measured). It was found that not all GULP libraries (force-fields) could reproduce these properties, although the ‘Catlow 1992’ and ‘Sauer 1997’ libraries were found to produce good results. These libraries were then used to study the all-silica forms of various ‘presumably auxetic’ zeolites. The simulations generally confirmed the conclusions reported in earlier studies, and in particular, the fibrous zeolites THO, NAT and EDI were once again shown to be auxetic in the (001) plane. A study was also performed aimed at assessing the effect of interstitial species on the mechanical properties of NAT where it was shown that these species reduce the auxetic effect. This is very significant as once again we have confirmed the potential of these materials as molecular level auxetics, and hopefully, these results will result in generating more interest into the fascinating materials which could be used in many practical applications (*e.g.* tuneable molecular sieves).

Keywords: Auxetic, Zeolites, negative Poisson’s ratio, mechanical properties

1. Introduction

Materials with a negative Poisson’s ratio (auxetics) undergo a lateral expansion upon being subjected to a uniaxial load. This property may appear at various metrological scales ranging from the nanoscale (molecular level) to the macroscale. Auxetic behaviour results in various improved characteristics which means that these materials may be exploited in many applications. This paper will look at nanoscale auxetics, *i.e.*, materials where the auxetic behaviour is

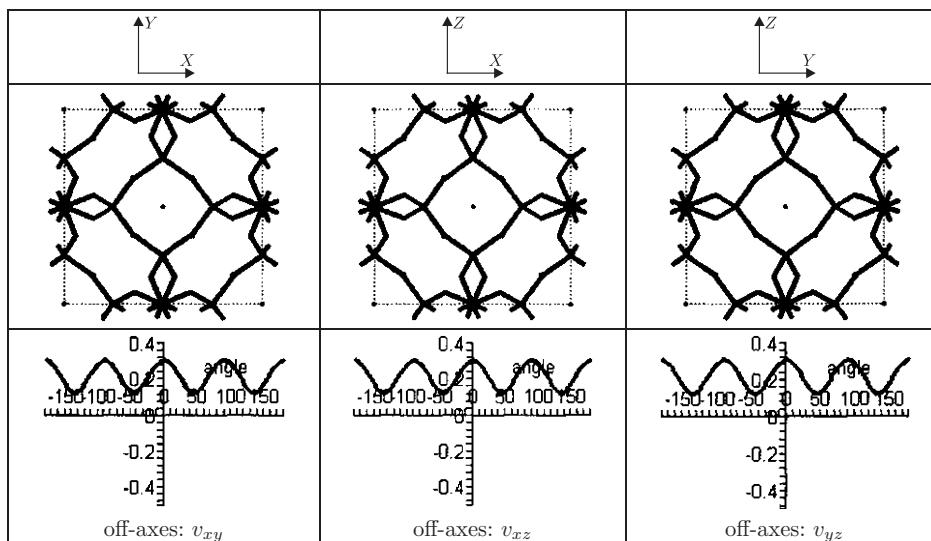
due to particular features at the material's nano (molecular) structure. It has been shown through modeling and/or experimental evidence that molecular level auxetic behaviour occurs in various classes of materials including polymers [1, 2], metals [3] and minerals [4–7]. Molecular modelling has played a very important role in this field.

In this paper we shall present the results of computer simulations of the mechanical properties of zeolites, in particular, for the zeolites for which other molecular modelling work has suggested that they may exhibit negative Poisson's ratio (for which no experimental mechanical properties data is available as yet). We use GULP libraries, involving the ion polarisability, to simulate the structure and the single crystalline mechanical properties of various zeolite frameworks for which negative Poisson's ratios were predicted using other force-fields (in particular various *Cerius*² force-fields, as Burchart, BKS, Universal and CVFF). We shall also study the effect of interstitial cations and water molecules on the mechanical properties.

We shall be performing two studies: (1) modelling of the 'empty' frameworks of the zeolites NAT, EDI, ABW, ATT, APD, AET, AHT, BIK, THO and JBW for which negative Poisson's ratios were predicted; (2) modelling of some of these frameworks with interstitial cations in an attempt to assess the effect of these species on the mechanical properties. We shall first test the methodology on the zeolite sodalite (SOD) for which experimentally determined mechanical properties are well known (Section 2). In Sections 3 and 4 we describe the results related to 'empty' and cation-containing frameworks, respectively. Finally Section 5 contain the conclusions for this study.

2. Modelling of sodalite

Sodalite, $\text{Na}_8[\text{Al}_6\text{Si}_6\text{O}_{24}]\text{Cl}_2$, is a naturally occurring aluminosilicate mineral that occurs in rock formation. The aluminosilicate framework is composed of SiO_4 and AlO_4 tetrahedra which share the corner oxygens in such a way that the aluminium and silicon atoms are completely ordered. The crystal lattice has $P4\ 3n$ symmetry. The crystal structure is characterised by cage-like cubo-octahedral units, bounded by six rings of four tetrahedra, parallel to the (100) plane and eight rings of six tetrahedra, parallel to the (111) plane. These six-membered rings form a set of channels, which intersect to give rise to large cavities. The chlorine atoms occupy these cavities, and are tetrahedrally coordinated with the sodium ions. Sodalite is characterised by being sodium rich and also in having chlorine as an essential constituent. The mechanical properties of sodalite have been determined experimentally by an ultrasonic method by Li and Nevitt [8] using a sodalite crystal 5 mm in diameter. The sound velocities through the sample were measured using the McSkimin-Fisher phase comparison method in the 20–75 MHz range, to ultimately give the elements of the stiffness matrix ($C_{11} = 88.52$ GPa, $C_{12} = 38.70$ GPa and $C_{44} = 36.46$ GPa, see Table 1).

Table 1. The structure and mechanical properties of sodalite as determined by Li *et al.* [8]

Cell parameters:

a	b	c	α	β	γ
8.890	8.890	8.890	90.000	90.000	90.000

On-Axes mechanical properties:

$C = [C_{ij}]$ [in GPa]	88.55	38.70	38.70	0.00	0.00	0.00
	38.70	88.55	38.70	0.00	0.00	0.00
	38.70	38.70	88.55	0.00	0.00	0.00
	0.00	0.00	0.00	36.46	0.00	0.00
	0.00	0.00	0.00	0.00	36.46	0.00
	0.00	0.00	0.00	0.00	0.00	36.46

E_x [GPa]	E_y [GPa]	E_z [GPa]	ν_{xy}	ν_{yx}	ν_{yz}	ν_{zy}	ν_{xz}	ν_{zx}
64.98	64.98	64.98	0.304	0.304	0.304	0.304	0.304	0.304

In this section we try to use GULP to simulate the single crystalline mechanical properties of sodalite and then we shall proceed to presenting our results and compare these to existing data. This will give us an indication of the suitability of the GULP libraries to model zeolites.

The mechanical properties of sodalite were experimentally determined for a crystal with composition $\text{Na}_8[\text{Al}_6\text{Si}_6\text{O}_{24}]\text{Cl}_2$. However:

- (1) None of the GULP libraries (*i.e.* the ‘Catlow 1992’ library [9–15], the ‘Parker 1992’ library [9, 16], the ‘Hope 1989’ library [17], the ‘Sauer 1997’ library [18, 19], the ‘Sastre 2003’ library [20] and the ‘glass’ library [21]) have been parameterised to deal with such system as they do not contain terms for Cl^- ;
- (2) The ‘Sastre 2003’ does not have parameters for Al^{3+} ;
- (3) Only the ‘Catlow 1992’ library contains parameters for Na^+ .

In view of this, we shall perform simulations on variants of the $\text{Na}_8[\text{Al}_6\text{Si}_6\text{O}_{24}]\text{Cl}_2$ system. In particular we will be modelling:

- (a) The SiO_2 equivalent of the $[\text{Al}_6\text{Si}_6\text{O}_{24}]^{6-}$ framework, *i.e.* $\text{Si}_{12}\text{O}_{24}$, which we shall refer to as SOD_SI (using all the six GULP libraries);
- (b) The $[\text{Al}_6\text{Si}_6\text{O}_{24}]$ framework which we shall refer to as SOD (using the six GULP libraries except the ‘Hope 1989’ and the ‘Sastre 2003’ libraries);
- (c) The $[\text{Al}_6\text{Si}_6\text{O}_{24}]$ framework with the eight Na^+ cations which we shall refer to as SOD_C (using all the ‘Catlow 1992’ libraries).

The models of SOD_SI, SOD and SOD_C were constrained with a $P\bar{4} 3n$ symmetry which is the symmetry of SOD. Not all simulations could be successfully performed. In particular, for all the systems modelled, no results could be obtained using the Hope and Sastre libraries even though these libraries were supposed to contain parameters for the simulations. This is because in the case of the Hope library the minimisation process failed (as was the case with α -cristobalite [22]) whilst in the case of the Sastre library, the program reported a ‘segmentation error’ during the minimisation. Moreover, in the case of the SOD model, the minimum energy configuration model was not outputted when using the glass library because the minimisation process failed to converge. In all the other cases, the simulations for the systems were performed to completion, and it was observed that:

- (a) There were no significant differences between the simulations with a with a $P\bar{4} 3n$ symmetry and those with a P1 symmetry (to the fourth significant figure), although the former were faster than the latter;
- (b) All the systems maintained its cubic symmetry and the same structure and mechanical properties in the XY , YZ and XY planes.

A summary of the results is provided in Table 2 to Table 8 where the GULP simulated properties are compared to the experimentally obtained properties and to the results from simulations produced by other authors, namely the work of Grima (2000) dedicated to modelling of the SOD_SI and SOD frameworks using the *Cerius*², Burchart, BKS, Universal and CVFF force-fields and the works of Wood [23] and Grima *et al.* [24] on modelling SOD_SI and SOD using the custom-made ZEO_FF2 force-fields (an altered version of the Burchart-Universal force-field) and for modelling of SOD_C using the Universal, CVFF and ZEO_FF2.

To help us quantify better the extent of the differences between the experimental properties and the simulated values (as obtained by the different GULP and *Cerius*² libraries / force-fields), we have graphically compared the magnitudes of the cell parameters ($a = b = c$), the on-axes Young’s moduli E , the on-axes Poisson’s ratios, ν_{ij} ($i, j = x, y, z$) and on-axes the shear moduli G (Figures 1–4).

These results clearly show that, when appropriate (*i.e.*, for the particular cases of SOD_SI and SOD) the ‘Catlow 1992’ and the ‘Parker 1992’ libraries produced very similar results for all structural and mechanical properties. Since

Table 2. The GULP simulated properties of SOD_SI

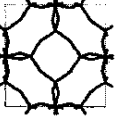
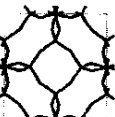
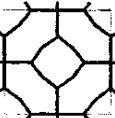
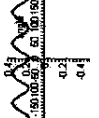
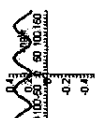
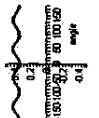
	CATLOW	PARKER	HOPE	SAUER	SASTRE	GLASS
structure in the XY plane			—		—	
off-axis plots of v_{xy}			—		—	
E_x (GPa)	78.68	78.67	—	63.00	—	155.51
v_{xy}	0.176	0.176	—	0.267	—	0.331
G_{xy} (GPa)	22.96	22.96	—	21.34	—	48.38

Table 3. Properties of SOD_SI from literature (* the experimental structure refers to $\text{Na}_8[\text{Si}_6\text{Al}_6\text{O}_{12}]\text{Cl}_2$)

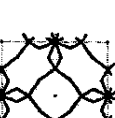
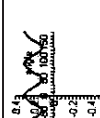
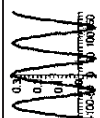
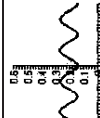
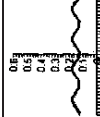
	EXPERIMENTAL*	BURCHART	BKS	UNIVERSAL	CVFF	ZEO_FF2
structure in the XY plane						
off-axis plots of v_{xy}						
E_x (GPa)	64.98	82.16	12.87	188.36	118.11	84.06
v_{xy}	0.304	0.233	0.318	0.147	0.124	0.238
G_{xy} (GPa)	36.46	23.63	10.99	63.76	47.41	21.65
ref.	Li et al. (1989)	Grima (2000)	Grima (2000)	Grima (2000)	Grima (2000)	Wood (2003)

Table 4. The GULP simulated properties of SOD

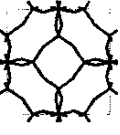
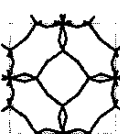
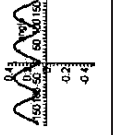
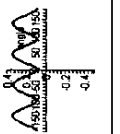
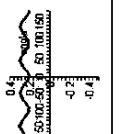
	CATLOW	PARKER	HOPE	SAUER	SASTRE	GLASS
structure in the XY plane			-		-	-
off-axis plots of v_{xy}			-		-	-
E_x (GPa)	64.91	64.91	-	49.81	-	-
v_{xy}	0.093	0.093	-	0.212	-	-
G_{xy} (GPa)	17.56	17.56	-	17.19	-	-

Table 5. Properties of SOD from literature (* the experimental structure refers to $\text{Na}_8[\text{Si}_6\text{Al}_6\text{O}_{12}]\text{Cl}_2$)

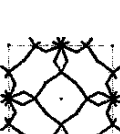
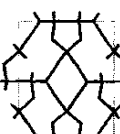
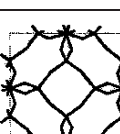
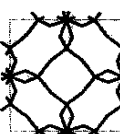
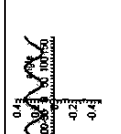
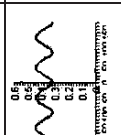
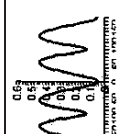
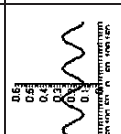
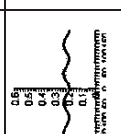
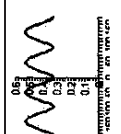
	EXPERIMENTAL*	BURCHART	BKS	UNIVERSAL	CVFF	ZEO_FF2
structure in the XY plane						
off-axis plots of v_{xy}						
E_x (GPa)	64.98	47.78	38.70	167.95	107.63	47.22
v_{xy}	0.304	0.323	0.049	0.110	0.194	0.328
G_{xy} (GPa)	36.46	13.60	11.98	55.64	41.29	10.85
ref.	Li et al. (1989)	Grima (2000)	Grima (2000)	Grima (2000)	Grima (2000)	Wood (2003)

Table 6. The GULP simulated properties of SOD_C

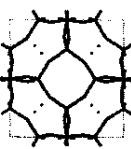
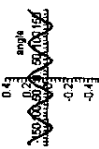
	CATLOW	PARKER	HOPE	SAUER	SASTRE	GLASS
structure in the XY plane		-	-	-	-	-
off-axis plots of v_{xy}		-	-	-	-	-
E_x (GPa)	81.62	-	-	-	-	-
v_{xy}	0.177	-	-	-	-	-
G_{xy} (GPa)	53.73	-	-	-	-	-

Table 7. Properties of SOD_C from literature (* the experimental structure refers to $\text{Na}_8[\text{Si}_6\text{Al}_6\text{O}_{12}]\text{Cl}_2$)

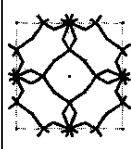
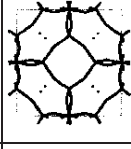
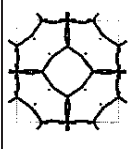
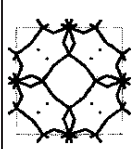
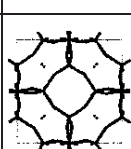
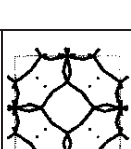
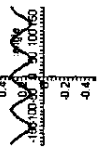
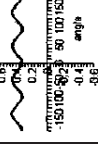
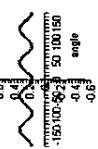
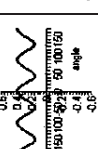
	EXPERIMENTAL*	BURCHART	BKS	UNIVERSAL	CVFF	ZEO_FF2
structure in the XY plane						
off-axis plots of v_{xy}						
E_x (GPa)	64.98	47.60	50.86	166.18	49.78	51.80
v_{xy}	0.304	0.326	0.373	0.166	0.389	0.344
G_{xy} (GPa)	36.46	13.30	17.99	50.16	29.70	14.92
ref.	Li et al. (1989)	Wood (2003)	Wood (2003)	Wood (2003)	Wood (2003)	Wood (2003)

Table 8. A summary of the mechanical and structural properties of the sodalite models

Structure	Method	$a = b = c$ [Å]	E [GPa]	ν	G [GPa]
$\text{Na}_8[\text{Si}_6\text{Al}_6\text{O}_{24}]\text{Cl}_2$	Experimental	8.890	64.98	0.304	36.46
SOD_SI	Catlow	8.767	78.68	0.176	22.96
	Parker	8.767	78.67	0.176	22.96
	Sauer	8.749	63.00	0.267	21.34
	Glass	9.083	155.51	0.331	48.38
	Burchart	8.666	82.16	0.233	23.63
	BKS	8.956	12.87	0.318	10.99
	Universal	8.029	188.36	0.147	63.76
SOD	CVFF	8.606	118.11	0.124	47.41
	ZEO_FF2	8.528	84.06	0.238	21.65
	Catlow	9.097	64.91	0.093	17.56
	Parker	9.097	64.91	0.093	17.56
	Sauer	9.098	41.89	0.212	17.19
	Glass	–	–	–	–
	Burchart	9.059	47.78	0.323	13.60
SOD_C	BKS	7.499	38.70	0.049	11.98
	Universal	8.106	167.95	0.110	55.64
	CVFF	9.176	107.63	0.194	41.29
	ZEO_FF2	8.920	47.22	0.328	10.85
	Catlow	9.164	64.91	0.093	53.73
	Parker	–	–	–	–
	Sauer	–	–	–	–
SOD_C	Glass	–	–	–	–
	UFF-Burchart	9.104	47.60	0.326	13.30
	Burt-Dreiding	9.138	50.86	0.373	17.99
	Universal	8.422	166.18	0.166	50.16
	CVFF	9.253	49.78	0.389	29.70
	ZEO_FF2	9.064	51.80	0.344	14.92

all of the simulations were performed on different (albeit similar) structures than the one for which experimental results are available, one would expect that the simulated values would differ from the experimental results. In fact, as illustrated in Table 8 and Figure 1 to Figure 3, we may observe that the differences between the GULP simulated structural properties / moduli and the equivalent experimental properties were larger than those observed in the earlier study on α -cristobalite [22] where we were comparing ‘like with like’. However, it should be noted that such trends were also observed with other published molecular modelling results (obtained using *Cerius*² force-fields) on

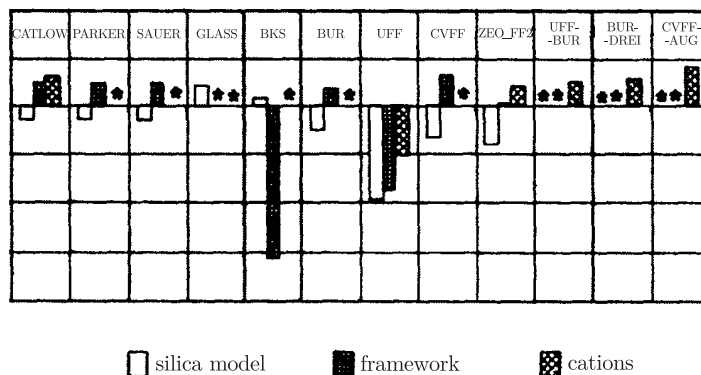


Figure 1. Deviation of the values for the cell parameters compared (* indicates that the parameter was not plotted)

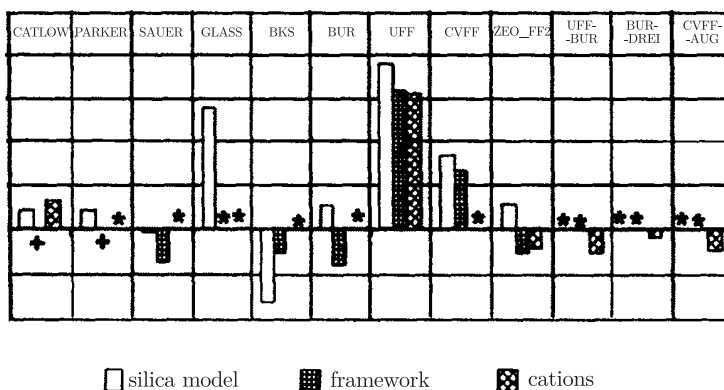


Figure 2. Deviation of the values for the Young's moduli compared (* indicates that the parameter was not plotted; + indicates that the parameter was plotted and the deviation is close to 0)

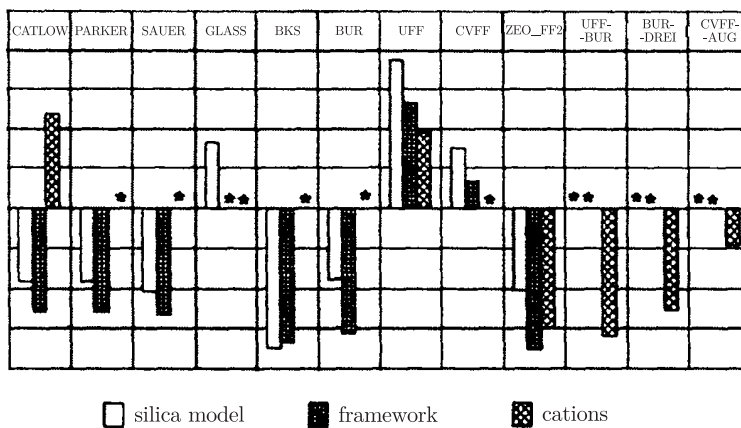


Figure 3. Deviation of the values for the shear moduli compared (* indicates that the parameter was not plotted)

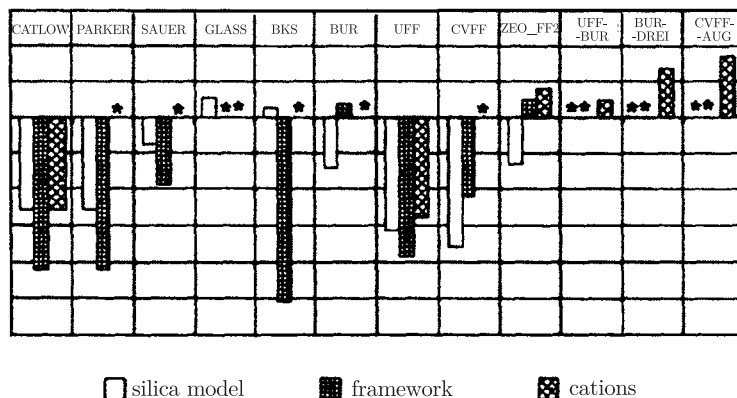


Figure 4. Deviation of the values for Poisson's ratios compared (* indicates that the parameter was not plotted)

sodalite, where in fact the observed deviations between experimental values for the cell parameters and Young's moduli were larger than when simulated using the 'Catlow 1992', 'Parker 1992' and 'Sauer 1997' libraries. It should also be noted that the minimum energy structure of SOD_SI obtained using the glass library (see Table 2) differed considerably from the experimentally determined structure of sodalite (see Table 1). In all the other cases, the GULP minimum energy structures were similar to the experimentally determined structure. In the case of the on-axes Poisson's ratios, the deviations between the experimental and GULP simulated values were smallest when using the 'Sauer 1997' library and the glass libraries, although the latter refer to a structure which deviates considerably from the real structure of sodalite. This means that the 'Sauer 1997' library is best for simulating the on-axes Poisson's ratios. In the case of the off-axes Poisson's ratios, it was observed that only the SOD_C structure as simulated by the 'Catlow 1992' library gave a correct off-axes plot for the Poisson's ratios (compare Table 6, column 1 with Table 1). All the other simulations gave off-axes plot for the Poisson's ratios which were out of phase by 45° (compare Table 2 and Table 4 with Table 1). This anomaly, however, was also evident in the simulations carried out using *Cerius*² force-fields and described in literature (see Table 3, Table 5 and Table 7).

From these simulations it may be concluded that:

- (1) The GULP libraries are not parameterised for a wide range of the periodic table, a property which limits their use. In this particular case sodalite could not be modelled as $\text{Na}_8[\text{Al}_6\text{Si}_6\text{O}_{24}]\text{Cl}_2$ as these libraries lack the parameters for Cl. Furthermore, only the Catlow 1992 library had the Na^+ parameters.
- (2) For soda lime, the imposition or otherwise of the P4 3n does not effect the results of the simulations.
- (3) The results obtained by the 'Catlow 1992', 'Parker 1992' and 'Sauer 1997' libraries were of equivalent quality (if not better) to those obtained in similar

simulations performed in previous studies by other workers using *Cerius*² force-fields. Of these:

- (a) The ‘Sauer 1997’ gave the best agreement for the Poisson’s ratios (SOD and SOD_SI *vs.* experimental data for Na₈[Al₆Si₆O₂₄]Cl₂). However, this library contains no parameters for Na⁺ and hence could not be used for simulating SOD_C.
- (b) The ‘Catlow 1992’ and ‘Parker 1992’ predicted the same properties for SOD and SOD_SI. However, data could not be obtained for SOD_C using the Parker library as this contains no parameters for Na⁺.

In view of all this, the ‘Sauer 1997’ and ‘Catlow 1992’ were found to be the most suitable libraries for performing simulation studies on the zeolite sodalite.

3. Modelling of zeolite frameworks

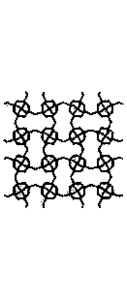
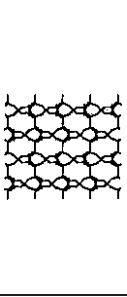
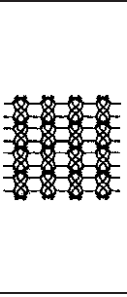
Force-field based molecular modelling simulations [7, 25, 23] using various *Cerius*² force-fields (Burchart, BKS, Universal and CVFF) have predicted that several zeolite frameworks and their SiO₂ equivalents, in particular NAT, EDI, ABW, ATT, APD, AET, AHT, BIK, THO and JBW exhibit negative Poisson’s ratios. In the mentioned works no cations or water molecules were included. Grima had also shown that the predictions made on the SiO₂ equivalents of the zeolites showed the same trends as those made on the empty ‘original’ zeolite frameworks.

In view of the results obtained in the previous section (*i.e.* that the Catlow and Sauer libraries can simulate the properties of the SiO₂ equivalent of the sodalite framework), we shall attempt to use the ‘Catlow 1992’ and the ‘Sauer 1997’ libraries to reproduce the mentioned predictions that the SiO₂ equivalents of the zeolites NAT, EDI, ABW, ATT, APD, AET, AHT, BIK, THO and JBW exhibit negative Poisson’s ratios. These libraries were chosen since the validation work indicated these as the best candidate libraries to use for simulating zeolites and zeolites-like structures. For all of these systems, the simulations were performed (i) with the symmetry of the framework being imposed and (ii) with a P1 symmetry. In this section, unless otherwise states, all reference to ‘zeolites’ will refer to ‘the SiO₂ equivalents of the zeolites’.

A summary of the structural and mechanical properties (the on- and off-axes Poisson’s ratios) for the ‘auxetic planes’ in the SiO₂ equivalents of the zeolites are presented in Table 9 to Table 19. These tables contain the results as simulated by GULP and by the *Cerius*² force-fields in the earlier studies by Grima [7] and Wood [23]. It should be noted that not all the simulations could be performed, or performed to completion successfully (*cf.* void panels in the Tables).

From the results in Table 9 to Table 19, it is evident that there were cases (in particular APO, ABW and AET) when there are significant differences between the properties as simulated with the imposed crystal symmetry and those simulated with a P1 symmetry. In other cases (in particular NAT, JBW, EOI and AHT) the two sets of results are identical or very similar. In the case of ABW, AET and APD, the difference in the results as arising from the presence or absence of the

Table 9. The simulated properties of THO_SI

		
XY-plane (X = horizontal)	XZ-plane (X = horizontal)	YZ-plane (Z = horizontal)

experimentally determined structure

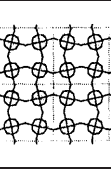
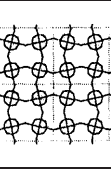
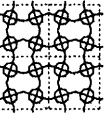
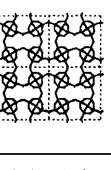
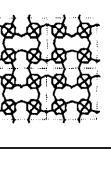
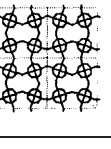
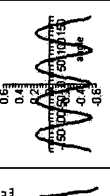
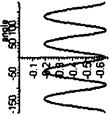
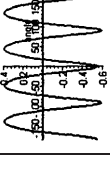
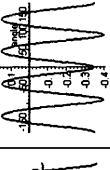
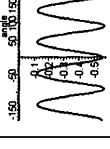
	CATLOW (P1)	SAUER (P1)	CATLOW (SYM)	SAUER (SYM)	BURCHART	BKS	UFF	CVFF
structure in the XY plane			—	—				
off-axis plots of v_{xy}			—	—				
v_{xy}	-0.630	-0.529	—	—	-0.64	-0.55	-0.35	-0.56
v_{yx}	-0.654	-0.550	—	—	-0.65	-0.59	-0.40	-0.57

Table 10. The simulated properties of EDI_SI

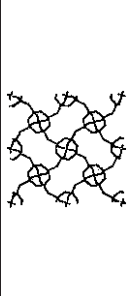
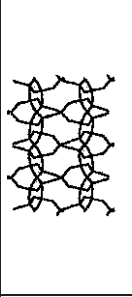
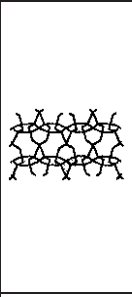
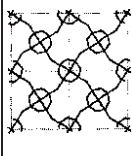
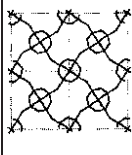
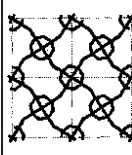
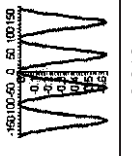
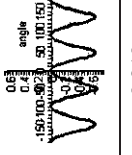
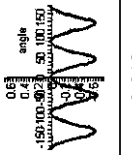
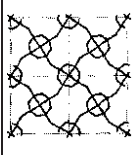
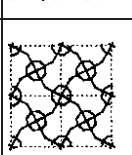
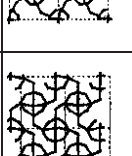
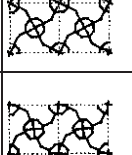
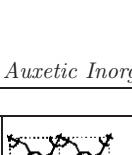
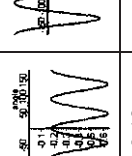
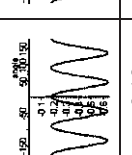
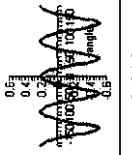
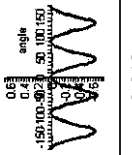
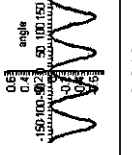
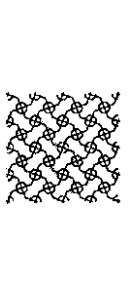
			
	XY-plane ($X = \text{horizontal}$)	XZ-plane ($X = \text{horizontal}$)	YZ-plane ($Z = \text{horizontal}$)
experimentally determined structure			
structure in the XY plane			
off-axis plots of v_{xy}			
v_{xy}	0.012	0.210	0.013
v_{yx}	0.012	0.210	0.013
			
			
			
			
			
			
			
			
			
			
v_{xy}			0.210
v_{yx}			0.210
			0.12
			0.47
			-0.18
			-0.18
			0.21
			0.21
			-0.10
			-0.10

Table 11. The simulated properties of NAT_SI

		
XY-plane (X = horizontal)	XZ-plane (X = horizontal)	YZ-plane (Z = horizontal)

experimentally determined structure

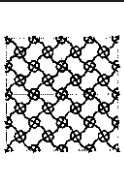
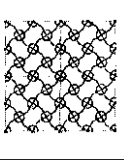
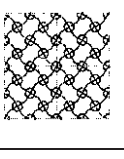
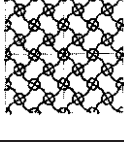
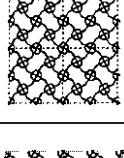
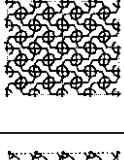
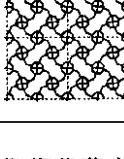
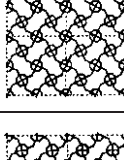
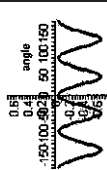
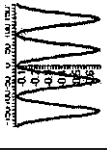
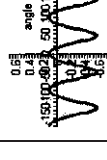
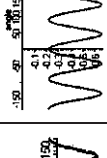
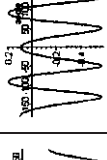
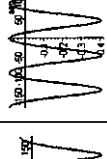
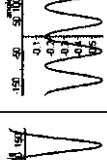
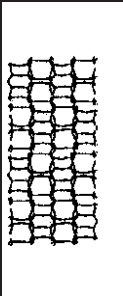
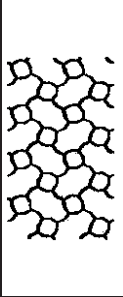
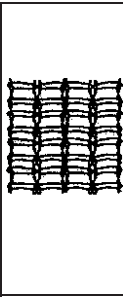
	CATLOW (SYM)	SAUER (SYM)	CATLOW (P1)	SAUER (P1)	BURCHART	BKS	UFF	CVFF
structure in the XY plane								
off-axis plots of v_{xy}								
v_{xy}	-0.056	0.122	-0.065	0.117	-0.22	0.10	0.09	-0.16
v_{yz}	-0.056	0.122	-0.065	0.117	-0.20	0.20	0.09	-0.16

Table 12. The simulated properties of APD_SI

		
XY-plane ($X = \text{horizontal}$)	XZ-plane ($X = \text{horizontal}$)	YZ-plane ($Z = \text{horizontal}$)

experimentally determined structure

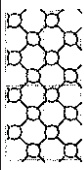
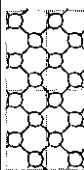
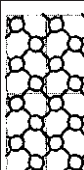
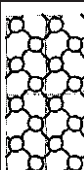
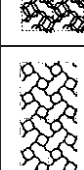
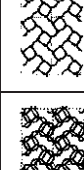
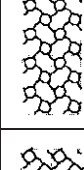
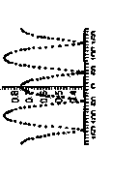
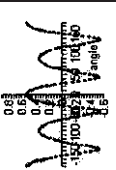
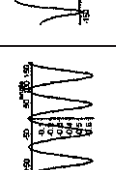
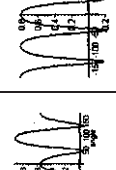
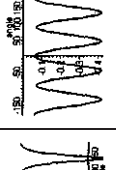
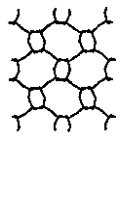
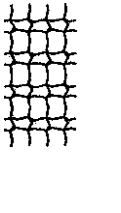
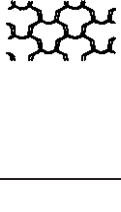
	CATLOW (SYM)	SAUER (SYM)	CATLOW (P1)	SAUER (P1)	BURCHART	BKS	UFF	CVFF
structure in the XY plane								
off-axis plots of v_{xy}			-					
v_{xy}	0.869	0.721	-	0.344	0.03	0.91	0.81	-0.07
v_{yx}	0.751	0.587	-	0.530	0.03	0.55	0.81	-0.06

Table 14. The simulated properties of ABW_SI

		
XY-plane (X = horizontal)	XZ-plane (X = horizontal)	YZ-plane (Z = horizontal)

experimentally determined structure

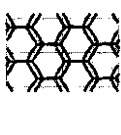
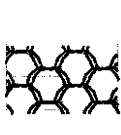
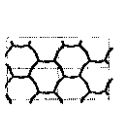
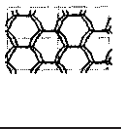
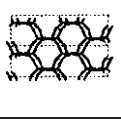
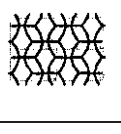
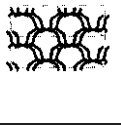
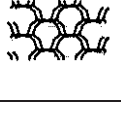
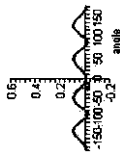
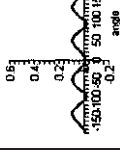
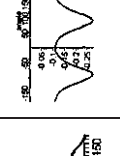
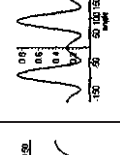
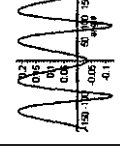
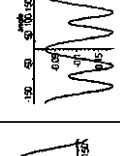
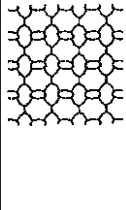
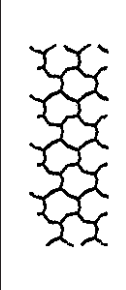
	CATLOW (SYM)	SAUER (SYM)	CATLOW (P1)	SAUER (P1)	BURGHART	BKS	UFF	CVFF
structure in the XY plane								
off-axis plots of v_{xy}								
v_{xy}	0.001	-0.009	-0.178	-0.009	-0.11	0.26	-0.04	-0.03
v_{yx}	0.001	-0.018	-0.370	-0.018	-0.28	0.85	-0.12	-0.08

Table 16. The simulated properties of JBW_SI

		
XY-plane (X = horizontal)	XZ-plane (X = horizontal)	YZ-plane (Z = horizontal)

experimentally determined structure

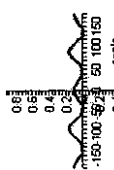
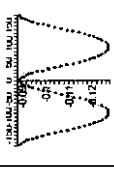
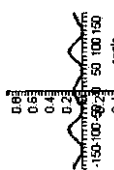
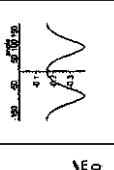
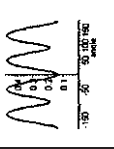
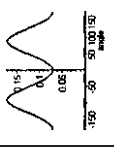
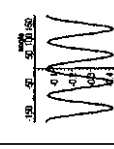
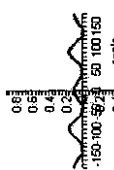
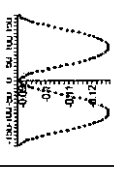
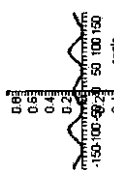
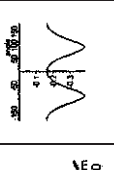
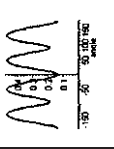
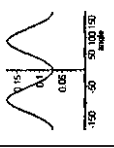
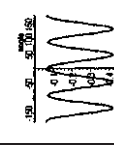
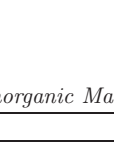
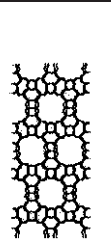
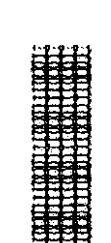
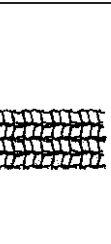
	CATLOW (SYM)	SAUER (SYM)	CATLOW (P1)	SAUER (P1)	BURCHART	BKS	UFF	CVFF
structure in the XY plane								
off-axis plots of v_{xy}								
v_{xy}	-0.129	0.160	-0.129	0.160	-0.38	0.19	0.17	-0.18
v_{yz}	-0.088	0.103	-0.088	0.103	-0.16	0.13	0.07	-0.02

Table 17. The simulated properties of AET_SI

		
XY-plane ($X = \text{horizontal}$)	XZ-plane ($X = \text{horizontal}$)	YZ-plane ($Z = \text{horizontal}$)

experimentally determined structure

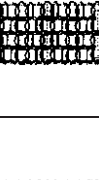
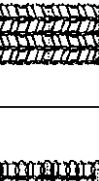
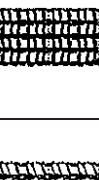
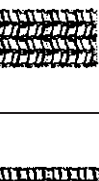
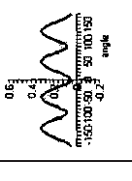
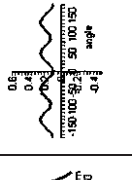
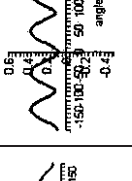
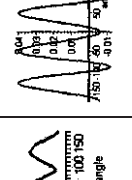
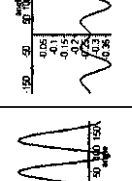
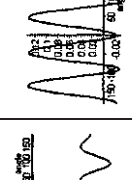
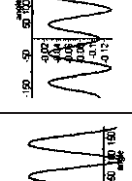
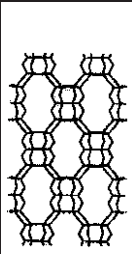
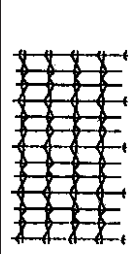
	CATLOW (SYM)	SAUER (SYM)	CATLOW (P1)	SAUER (P1)	BURCHART	BKS	UFF	CVFF
structure in the XY plane								
off-axis plots of v_{xy}								
v_{xy}	-0.046	0.056	0.099	0.083	-0.01	-0.28	-0.02	-0.11
v_{yx}	-0.072	0.085	0.127	0.115	-0.01	-0.37	-0.03	-0.13

Table 18. The simulated properties of AHT_S1

		
XY-plane (X = horizontal)	XZ-plane (X = horizontal)	YZ-plane (Z = horizontal)

experimentally determined structure

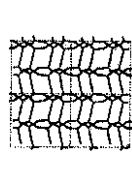
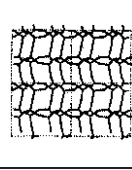
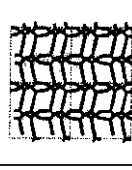
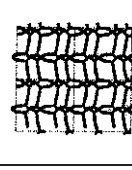
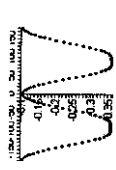
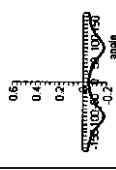
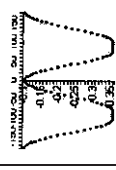
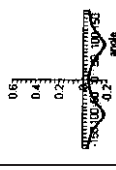
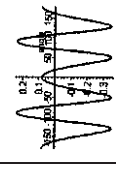
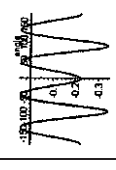
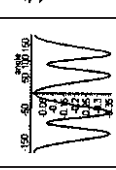
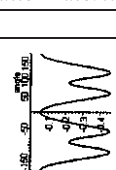
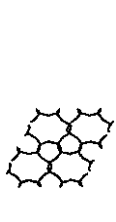
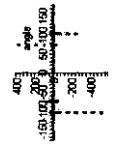
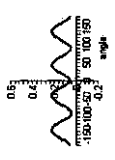
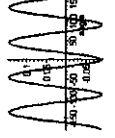
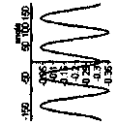
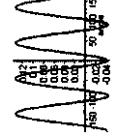
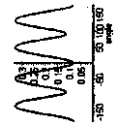
	CATLOW (SYM)	SAUER (SYM)	CATLOW (P1)	SAUER (P1)	BURCHART	BKS	UFF	CVFF
structure in the XY plane								
off-axis plots of v_{xy}								
v_{xy}	-0.104	-0.049	-0.104	-0.049	0.08	-0.23	-0.01	-0.05
v_{yx}	-0.359	-0.176	-0.359	-0.176	0.24	-0.34	-0.07	-0.22

Table 19. The simulated properties of BIK-SI

		
XY-plane ($X = \text{horizontal}$)	XZ-plane ($X = \text{horizontal}$)	YZ-plane ($Z = \text{horizontal}$)

experimentally determined structure

	CATLOW	SAUER	—	—	BURCHART	BKS	UFF	CVFF
structure in the XY plane			—	—				
off-axis plots of v_{xy}			—	—				
v_{xy}	-0.494	0.058	—	—	-0.09	-0.32	-0.04	0.08
v_{yz}	1.862	0.046	—	—	-0.09	-0.36	-0.04	0.11

symmetry constraints was due to the fact that the minimisations did not result in the generation of the same minimum energy conformation. Instead the two processes (with symmetry and without symmetry) resulted in systems relating to two different local minima. This poses a question as to which of the two sets of results is more credible. In such cases, the normal criteria that are used for choosing the more credible set of results are: (i) which of the two systems has the least energy; (ii) which of the two simulated systems has a minimum energy structure which is closest to the experimentally obtained structure. Unfortunately, the two different minimum energy systems had very similar energies. The results from second criterion could also be misleading as the systems we are modelling are SiO_2 systems whilst the experimentally obtained structures contained aluminium and/or phosphorus in the framework together with other interstitial ions and water molecules. In view of all this, both sets of systems will be analysed. It should also be noted that the results as obtained by the Catlow and Sauer libraries were not always identical although in some cases they predicted the same general trends whilst in others they did not. Once again, in such cases, unless it is obvious that one of the minimum energy structures is very different from the experimentally obtained structures, then the results as obtained by both libraries will be analysed.

Bearing all this in mind, and comparing the results obtained from our simulations with those obtained by the earlier study using the *Cerius*² force-fields [7], we found that:

- (a) Negative Poisson's ratios were confirmed by both the Catlow and Sauer libraries for the SiO_2 equivalents of the fibrous zeolites THO (in the XY -plane), EDI (in the XY -plane) and NAT (in the XY -plane). This is very significant as these XY -planes of these natrolite-related structures are characterised by a geometry which may be described in terms of 'rotating squares' [7] and hence this work is once again confirming the important role of this geometry for generating auxetic behaviour.
- (b) Negative Poisson's ratios have also been confirmed in the SiO_2 equivalents of the zeolites ABW (in the XY -plane and in the YZ -plane) and AHT (in the YZ -plane)¹ by both the Catlow and Sauer libraries. Note that in the case of ABW (XY -plane), the Catlow results of the simulations with and without symmetry very different from each other, and only the simulations where symmetry was imposed resulted in negative Poisson's ratios. This is discussed below.
- (c) The negative Poisson's ratios in the SiO_2 equivalents of the zeolite JBW (in the XY -plane) and were confirmed by the Catlow libraries whilst the Sauer library gave low positive Poisson's ratios. Also, the negative Poisson's ratios in the SiO_2 equivalents of the zeolite APD (in the XZ -plane) was only confirmed

1. In the case of AHT (YZ -plane), the GULP libraries predicted negative Poisson's ratios but the off-axis plots were different to those simulated by the *Cerius* force-fields.

- by the Sauer library with a P1 symmetry whilst when symmetry constraints were imposed, the Catlow and Sauer library gave low-positive Poisson's ratios.
- (d) The negative Poisson's ratios in the SiO_2 equivalents of the zeolites ATT (in the XZ -plane) were not confirmed by both libraries but these still predicted the same profile for the off-axes plots as was previously obtained by the *Cerius*² force-fields when negative Poisson's ratios were predicted. The positive Poisson's ratios for these two zeolites are discussed below.
- (e) Inconclusive results were obtained for the zeolites AET and BIK (in the YZ -plane) in which cases the earlier predictions could not be confirmed since:
- In the case of AET, negative Poisson's ratios were predicted by the Catlow library with the imposed symmetry but high positive Poisson's ratios were obtained when the Catlow library was used with a P1 version of AET and when the Sauer library was used.
 - In the case of BIK, the Sauer library produced high positive Poisson's ratios whilst in Catlow library produced results which were very different from those produced by the other methods, but still exhibits negative Poisson's ratios for loading in some directions.

It is interesting to note that the only zeolite for which all the GULP simulations suggest that is non-auxetic was ATT (in the X -plane), and in this case this different result can be explained in terms of the differences in the geometry of the minimum energy conformation obtained by the GULP libraries when compared to those obtained by the *Cerius*² force-fields. In this case, the *Cerius*² force-fields produced minimum energy configurations where projections of the nanostructure of the zeolites in plane in which negative Poisson's ratios were predicted could be described in terms of partially-open 'rotating squares' (see Figure 5 a) but in the case of the GULP libraries, these squares appear in their fully open position (see Figure 5 b). In the idealised scenario where the 'rotating squares' are perfectly rigid, this system would be much more stiff (the stiffness of the idealised 'rotating squares' system increases as the structure opens up, reaching an infinite stiffness at the fully open position) but would still be auxetic with Poisson's ratios of -1 . However, as Grima [7] has suggested, if the squares are not perfectly rigid (as is the case in real materials), then such systems are likely to become less auxetic as the resistance to 'rotations' increases (something which happens when the angle between the squares increases). The loss of the auxetic behaviour occurs due to the fact that in such cases, the deformation of the squares would start to take precedence over rotations (*i.e.* the squares would tend to deform more than they would rotate). Grima [7] argues that in such systems where an alternative deformation mechanism starts to become more pronounced, one would still be able to identify some general characteristics of the original deformation mechanism. Our simulations on ATT suggest that what we have described seems to have happened since we can still observe that for the GULP simulated structures, the lowest Poisson's ratios are obtained when loading in the directions which correspond to the major axis of the 'rotating squares'

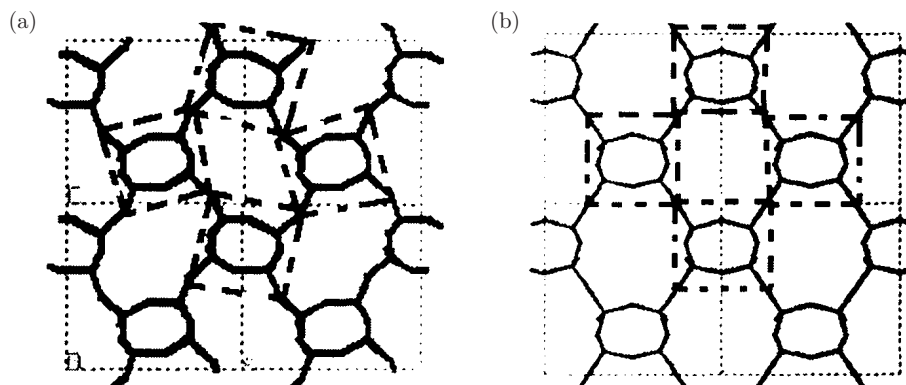


Figure 5. The projection minimum energy conformations of ATT in the XZ -plane with the ‘squares’ highlighted. These conformations were obtained by (a) the Burchart force-field in *Cerius²*, and (b) the GULP libraries

model (*i.e.* at 45° to the main X & Z axis). This is very well illustrated by the retention of the shape for the graphs of the off-axes Poisson’s ratios by the GULP libraries.

Further evidence that the loss of the auxetic behaviour is due to the fact that the ‘squares’ are now in their fully open position can be obtained by looking at the Catlow simulations for ABW (looking at the xy -plane). If we look at the xy -plane of this zeolite, we observe that whilst the minimisation with the imposed symmetry results in a system which may be described by ‘partially open rotating squares’, the system with a P1 symmetry results in a geometry which is describable as a ‘full open rotating squares’ system. These two systems (which correspond to two local minima of the same structure) exhibit very different properties and the former (*i.e.* the ‘partially open rotating squares’ system) exhibits auxetic behaviour whilst the latter (*i.e.* the ‘full open rotating squares’ system) does not. Similar results were also obtained for APD (in the XZ -plane) using the Sauer library although this time, the auxetic system which has the ‘partially open rotating squares’ geometry is the one obtained using P1 symmetry whilst the non-auxetic system which has the ‘fully open rotating squares’ geometry is the one obtained using symmetry constraints. All this is very significant as it illustrates the dependence of the Poisson’s ratios on the nanostructure of the materials and the way the nanostructure deforms when subjected to loads.

From these results it can be concluded that the predictions that some zeolites exhibit negative Poisson’s ratios have been confirmed through these new core-shell simulations. In particular it has been shown that the SiO_2 equivalents of the fibrous zeolites THO, EDI and NAT have always been predicted to exhibit negative Poisson’s ratios, thus confirming the important role of the ‘rotating squares’ mechanism for generating auxetic behaviour. The simulations also confirm the fine dependence of the Poisson’s ratios on the nanostructure of the materials and the way the nanostructure deforms when subjected to loads. In fact, we have

shown that a slight modification in the structure as a result of the way a system minimises could result in loss of the auxetic behaviour, as was observed in the case of ATT.

4. Modelling the effect of interstitial species on the Poisson's ratios in auxetic zeolites

Studies of Grima & Wood [24] and Wood [23] have indicated that the auxetic behaviour that is observed in zeolite frameworks is reduced by the presence of interstitial cations and water molecules. While zeolites can easily be dehydrated to remove the interstitial water molecules, interstitial cations are much more difficult to remove and thus this warrants investigation. In this section, we will attempt to use GULP to obtain a clearer picture on the effect of interstitial species on the mechanical properties of selected zeolite – the sodium salt of the aluminosilicate $\text{Na}^+_{16}[\text{Al}_6\text{Si}_{24}\text{O}_{80}]$ (NAT). NAT is an excellent candidate for such study since all the simulations performed so far on the SiO_2 equivalent of the NAT framework suggest that this framework exhibits negative Poisson's ratios irrespective of the methodology used to model it. The auxetic behaviour in this zeolite has been explained in terms of the well documented 'rotating squares model' [7, 26, 27, 24] – a simple model based on the geometry of the nanostructure of this zeolite and way this nanostructure deforms when subjected to uniaxial loads. Furthermore, a preliminary study on the role of cations / water inside this particular zeolite framework has already been performed so any results obtained by GULP will be extremely valuable since they could add more weight to the hypothesis formulated after the preliminary study [23, 24] that the presence of cations / water in the framework leads to a reduction in the auxeticity.

We performed simulations on two types of systems, namely on (a) the empty NAT aluminosilicate framework (referred to as NAT_AL), and (b) the NAT aluminosilicate framework with the Na^+ cations (referred to as NAT_C), using symmetry constraints and with a P1 symmetry. The results are presented in Tables 20 and 21. The tables contain images of the XY-plane of the minimum energy structures and the simulated Poisson's ratios in these planes. Corresponding data on the NAT_SI system, discussed in the previous Section, are also shown in the Tables.

The results clearly show that whilst there is little difference between the properties of NAT_SI and NAT_AL, there is a sizeable decrease in auxetic behaviour upon including the cations. There was also significant increase in the Young's moduli of the systems indicating that the presence of the cations makes the zeolite less pliable. This confirms the earlier preliminary study, where it was shown (through force-field based simulations at various uniaxial loads) that the reason for this decrease in auxetic behaviour is that while the 'rotating squares' mechanism is still present, the interstitial species interact with the framework causing it to become more stiff and rigid. It is also important to note, however, that the system remains auxetic, despite the addition of cations.

Table 20. Catlow simulated properties of NAT in P1 symmetry

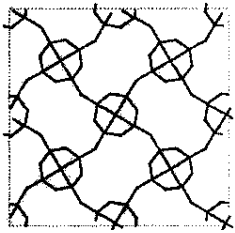
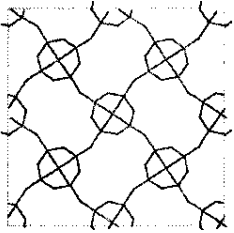
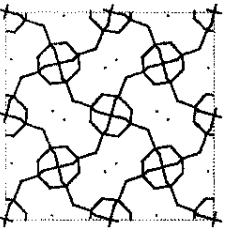
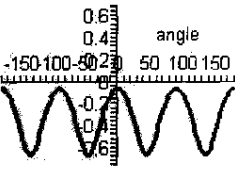
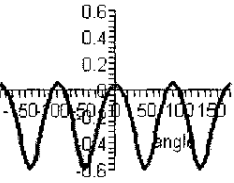
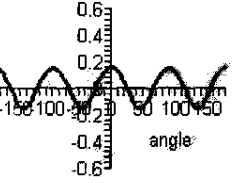
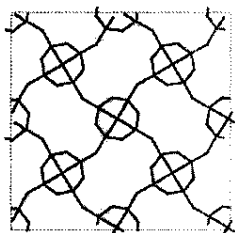
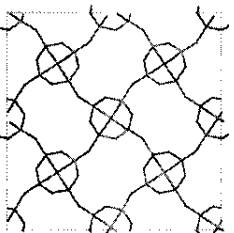
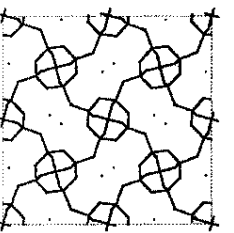
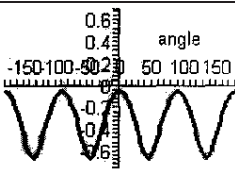
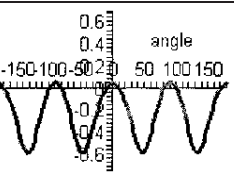
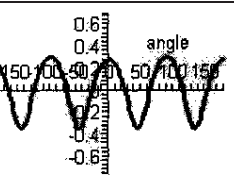
SILICA MODEL	FRAMEWORK MODEL	CATION MODEL
		
		
off-axes: v_{xy} NAT_SI v_{xy} -0.065 v_{yx} -0.065	off-axes: v_{xy} NAT v_{xy} 0.038 v_{yx} 0.082	off-axes: v_{xy} NAT_C v_{xy} 0.159 v_{yx} 0.257

Table 21. Catlow simulated properties of NAT with symmetry constraints

SILICA MODEL	FRAMEWORK MODEL	CATION MODEL
		
		
off-axes: v_{xy} NAT_SI v_{xy} -0.056 v_{yx} -0.056	off-axes: v_{xy} NAT v_{xy} 0.034 v_{yx} 0.047	off-axes: v_{xy} NAT_C v_{xy} 0.274 v_{yx} 0.305

From the results it may be concluded that the GULP Catlow library suggests that for NAT, the addition of interstitial cations in the model results in a less pronounced auxetic behaviour. This adds weight to previous work [23, 7] which has also reported such results. It should be noted that it would have been desirable that simulations could have been performed on more zeolites as such study could indicate whether this trend occurs in all zeolites (or at least in all fibrous zeolites) or just in NAT.

5. Conclusions

In this paper we have simulated the structures and elastic constants of:

- (1) Systems based on the zeolite sodalite for which the elastic constants have been experimentally measured;
- (2) The SiO₂ equivalents of the zeolites NAT, EDI, ABW, ATT, APD, AET, AHT, BIK, THO and JBW variants (which were predicted to potentially exhibit negative Poisson's ratios);
- (3) The zeolite NAT with and without interstitial cations in an attempt to study the effect of interstitial species on the Poisson's ratios.

In the case of (1) we have found that three GULP libraries, namely the Catlow library, the Parker library (which can be treated as a sub-set of the Catlow library) and the Sauer library produced minimum energy structures and Young's moduli which were in excellent agreement with the equivalent experimentally obtained values. It is interesting to note that for these inorganic minerals, the agreement of the simulated data to the experimental data was very dependent on the libraries used, and overall, there was not a major improvement in precision by including the ion polarisability. This suggests that a 'core-shell' model is not essential for simulating such minerals: being relatively small species, the polarisability in Si-O is not very important. Irrespective of all this, in case (2) we were able to confirm the predictions made by Grima [7] that some zeolite frameworks exhibit negative Poisson's ratios. In particular it has been shown that the SiO₂ equivalents of the fibrous zeolites THO, EDI and NAT have always been predicted to exhibit negative Poisson's ratios. Previous modelling work has suggested that these zeolites exhibit negative Poisson's ratios through a mechanism which may be trivially described in terms of a 'rotating squares' mechanism. It is interesting to observe that the GULP simulations have once again suggested that the directions of loading to achieve for maximum auxeticity corresponds to the directions of the 'major axis' of the a 'rotating squares' model. This is very significant as it confirms the important role of the 'rotating squares mechanism' for generating auxetic behaviour. Finally, in the case of (3), our results also confirmed the work of Wood [23] in confirming that for the fibrous zeolite NAT, auxetic behaviour is reduced by the presence of interstitial cations.

References

- [1] Griffin A C *et al.* 1998 *Macromolecules* **31** (9) 3145
- [2] Grima J N, Evans K E 2000 *J. Mat. Sci. Lett.* **19** 1563
- [3] Baughman R H 1998 *Nature* **392** 362
- [4] Yeganeh-Haeri A *et al.* 1992 *Science* **257** 650
- [5] Keskar N R, Chelikowsky J R 1993 *Phys. Soc. Cond. [??]* **16** 227
- [6] Alderson A *et al.* 2001 *AI Chem. Eng J.* **47** 2623
- [7] Grima J N 2000 *New Auxetic Materials, Ph. D. Thesis, University of Exeter*
- [8] Li Z *et al.* 1989 *Appl. Phys Lett.* **55** (17) 1730
- [9] Sanders M J, Leslie M J, Catlow C R A 1984 *J. Chem. Soc. Chem. Commun* [vol?] 1271
- [10] Jackson R A, Catlow C R A 1988 *Mol. Sim.* **1** 207

- [11] Schroder K P, Sauer J, Leslie M, Catlow C R A, Thomas J M 1992 *Chem. Phys. Lett.* **188** 320
- [12] Gale J D, Henson N J 1994 *JCS Faraday Trans.* **90** 3175
- [13] Jentys A, Catlow C R A 1993 *Catalysis Lett.* **22** 251
- [14] Lewis D W, Catlow C R A, Sankar G, Carr S W 1995 *J. Phys. Chem.* **99** 2377
- [15] den Ouden C J J, Jackson R A, Catlow C R A, Post M F M 1990 *J. Phys. Chem.* **94** 5286
- [16] Baram P S, Parker S C 1996 *Phil. Mag. B* **73** (1) 49
- [17] Hope A T J, Lengand C A, Catlow C R A 1989 *Proc. R. Soc. Lond A* **424** 57
- [18] Sierka M, Sauer J 1997 *Faraday Discuss.* **106** 41
- [19] Sauer J, Schroder K P, Termath V 1998 *Collect. Czech. Chem. Commun.* **63** 1394
- [20] Sastre G, Gale J D 2003 *Chem. Mater.* **15** 1788
- [21] Blonski S, Garofalini S H 1997 *J. Am. Ceram. Soc.* **80** 1997
- [22] Grima J N, Gatt R and Zammit V 2005 *Xjenza* **10** 24
- [23] Wood M 2003 *Molecular modelling of zeolites with negative Poisson's ratios*, B. Sc. Thesis, University of Malta
- [24] Wood M, Alderson A, Evans K E, Grima J N 2004 *Molecular modelling of auxetic zeolites*, NCS
- [25] Grima J N 2005, private communication
- [26] Grima J N, *et al.* 2000 *Acta Materialia* **48** 4349
- [27] Grima J N, Jackson R, Alderson A, Evans K E 1912 *Adv. Materials* **12**

